



# LABORATORI NAZIONALI DI FRASCATI

## SIS-Pubblicazioni

**LNF-02/023(P)**  
18 Ottobre 2002

### **The DEAR Kaon Monitor at DAΦNE**

V. Lucherini<sup>3</sup>, A. M. Bragadireanu<sup>3,4</sup>, G. Beer<sup>2</sup>  
C. Curceanu (Petrascu)<sup>3,4</sup>, J.-P. Egger<sup>5</sup>, C. Guaraldo<sup>3</sup>,  
M. Iliescu<sup>3,4</sup>, T. Ponta<sup>4</sup>, D. L. Sirghi<sup>3,4</sup>,  
F. Sirghi<sup>3</sup> and J. Zmeskal<sup>1</sup>

- <sup>1)</sup> *Institute for Medium Energy Physics, Boltzmannngasse 3,  
A-1090 Vienna, Austria*
- <sup>2)</sup> *Department of Physics and Astronomy, University of Victoria,  
P. O. Box 3055 Victoria B. C. V8W 3P6, Canada*
- <sup>3)</sup> *INFN, Laboratori Nazionali di Frascati, C. P. 13,  
Via E. Fermi 40, I-00044 Frascati, Italy*
- <sup>4)</sup> *Department of Elementary Particles Physics, Institute of Physics and  
Nuclear Engineering "Horia Hulubei",  
P.O. Box R-76900 Magurele, Bucharest, Romania*
- <sup>5)</sup> *Institute de Physique, Université de Neuchâtel,  
1 rue A. -L. Breguet, CH-2000 Neuchâtel, Switzerland*

### **Abstract**

Characteristics and performance of the kaon monitor of the DEAR experiment at the DAΦNE collider of Laboratori Nazionali di Frascati are described. The full TDC and ADC information collected from the detectors of the setup allows a clean observation of the charged kaon pairs from  $\phi$ -decay by means of their different arrival times with respect to the background particles. The number of detected kaons can be used to obtain an absolute luminosity measurement in the DEAR interaction point at DAΦNE.

PACS:14.40.Aq; 29.40.Mc; 29.20.Dh

To appear in Nuclear Instruments and Methods in Physics Research A

## 1 Introduction

The DEAR (DAΦNE Exotic Atom Research) experiment aims to perform precision measurements of *kaonic atom* characteristics, in order to obtain information on fundamental interactions. In particular, the experiment aims to determine the kaon-nucleon scattering lengths from a measurement of the position and width of the  $2p \rightarrow 1s$  x-ray transition in kaonic hydrogen and kaonic deuterium. The absolute yields of kaonic atom transitions can also be measured, allowing one to understand the underlying interatomic cascade mechanism. For this purpose, the experiment must be capable of counting the incident kaon flux.

The negative “kaon beam” used by DEAR is produced by the Frascati collider DAΦNE. The machine, optimized in luminosity for a center of mass energy of 1020 MeV in order to efficiently generate  $\phi$  (1020)-mesons, turns out to be a unique factory of low-energy charged kaons due to the large branching ratio (0.492) for  $\phi$ -decay into charged kaon pairs.

Since the  $\phi$ -resonance is produced almost at rest at DAΦNE, the charged kaons are emitted back-to-back with the same low momenta (127 MeV/c), experimental characteristics appealing for a selective tagging of events.

For a detailed description of the DEAR experiment and the DAΦNE collider, see ref.[1] and [2], respectively.

A dedicated monitor to detect the charged kaon flux from the DEAR interaction point of DAΦNE (IP2) was designed, built and is now operating. The monitor also satisfies specific machine requests. It can provide an absolute measurement of the luminosity delivered in IP2, with a substantial advantage with respect to conventional luminosity monitors which rely on processes (like beam-beam Bremsstrahlung or Bhabha scattering) having a smooth behavior with energy. The rate of kaon production is directly related to the tune of the machine energy to the  $\phi$ -resonance (4 MeV FWHM). Therefore, the Kaon Monitor can also be used to optimize the energy setting of the collider.

The monitor must provide a luminosity measurement simultaneously with DEAR data taking; hence the detector must fit in the small and crowded region of IP2 without interfering with the experiment. Moreover, it has to be a simple and reliable device which provides a reasonable counting rate for the luminosities reached at DAΦNE.

A set of thin scintillator slabs placed on opposite sides of the beam pipe at IP2, able to detect low energy back-to-back-correlated charged kaon pairs was realized. Simultaneous detection of  $K^+K^-$  pairs minimizes accidental events seen in a simple one-arm setup. Thickness, dimensions and positions of the scintillators were determined using a Monte Carlo simulation of all the processes involved.

In this paper, the experimental setup built for the DEAR Kaon Monitor is described. Its performance and experimental results are reported. In Sections 2 and 3 the experimental details of the Kaon Monitor setup and its operating method are given, while in the 4th Section the experimental results are presented and in Section 5 it is shown how the experimentally measured kaons provide on-line luminosity measurements. In Section 6 the conclusions from several weeks of operation of the monitor are summarized.

## 2 The Kaon Monitor setup

Since the DEAR experimental platform is placed above the beam pipe at IP2 of DAΦNE, the region at disposal for the Kaon Monitor lies in the radial plane of the machine. Other design considerations to be taken into account are:

- the free space along the beam pipe axis ( $\underline{z}$ -axis) is about 60 cm - the pipe is 90 mm diameter and the platform is placed 7 mm above the pipe ( $\underline{y}$ -axis);
- the (one standard deviation) dimensions of the crossing beams at IP2 are: 3 cm in  $\underline{z}$ , 2 mm in  $\underline{x}$ , 20  $\mu\text{m}$  in  $\underline{y}$ , respectively;
- the angular distribution of the charged kaons is isotropic in azimuth, but follows a  $\sin^2\theta$  law with respect to the  $\underline{z}$ -axis, implying a preferred normal emission with respect to the pipe.

The identification of the charged kaon pairs from  $\phi$ -decay is based on the specific characteristics of such kaons: low momentum and back-to-back topology (features only slightly altered by the thin DEAR beam pipe constructed of 250  $\mu\text{m}$  aluminum, reinforced by 650  $\mu\text{m}$  of carbon fiber). A “true” event is one in which both scintillator slabs fire in coincidence and which has the correct timing and energy loss (amplitude) information: i.e., the delay time and energy deposition typical of a non-relativistic charged particle.

The unwanted processes are: other decay channels of the  $\phi$  into charged particles; charged particles coming from the decay of neutral particles and, mainly, electromagnetic showers generated in the pipe and in the setup by the interaction of the 510 MeV electrons and positrons lost from the circulating beams. All these processes have in common a specific feature: the particles produced are fast and minimum ionizing (MIPs), in contrast to the charged kaons, which are slow and highly ionizing. Quantitatively, the charged kaons arrive *later* than the MIPs - approximately 1-2 ns - and deposit almost one order of magnitude more energy (for MIPs hitting the thin scintillator slabs normally).

All these design and physics considerations, including also the lifetime of charged kaons, multiple scattering and energy losses in materials and the overall geometrical constraints in IP2 were used as input parameters for a Monte Carlo simulation to select the

configuration for the monitor. The use of fast scintillators and fast phototubes was assumed, since time resolution is a crucial factor for the detector performance.

In summary, the configuration selected for the Kaon Monitor consists of two fast NE104 scintillator slabs, each 2 mm thick. Both scintillators are 8 cm high ( $y$ -axis) and 15 cm long ( $z$ -axis) and are placed back-to-back at IP2, on the two sides of the beam pipe, with the longest side parallel to it and are referred as the “inner” and the “outer” scintillator with respect to the center of the machine. The slabs are perpendicular to the machine radial plane. The back-to-back topology results in a background reduction by a factor of about 200. Each scintillator is seen by two fast XP2020 phototubes (PMs) mounted at the ends of each slab. By the use of a standard mean time technique, this configuration improves the time resolution, since it eliminates the differences in timing due to the distribution of impact points along the scintillators.

Each phototube is coupled to the scintillator by a short 45 degree tilted light guide, glued to the narrow side of the scintillator (80 x 2 mm). The bend was necessary to place the scintillators below the DEAR platform, in the available space between the last two focusing quadrupoles which face the interaction point. All PMs have a  $\mu$ -metal shield to protect them from the stray magnetic field. The loss in light transmission of such geometry gave no problem due to the high ionizing power (and hence high light yield) of the slow kaons near the end of their range, where 3 mm of scintillator stops them.

The Kaon Monitor experimental setup is shown schematically in Fig. 1, while Fig. 2 shows the scheme of the front-end electronics.

Analog signals from the anode of each phototube are passively split. One output is sent to a Lecroy 2249A CAMAC ADC for amplitude analysis; the other is sent to an ORTEC 935 Quad NIM 200 MHz Constant Fraction Discriminator (CFD). One of the two outputs from the CFD is sent to a CAEN C414 CAMAC TDC; the other is sent to a CAEN N235 NIM Dual Mean Timer. The trigger logic requires a coincidence between the “inner” and “outer” outputs of the Mean Timer. The output signal of the coincidence is sent to the gate of the CAMAC ADC. The veto output is used to inhibit a second discriminator fed by the Radio Frequency (RF) signal of the machine, the output of which gives the START to the TDC, as described below.

## 2.1 Timing procedure

In a multi-bunch collider such as DAΦNE, in which up to 120 bunches can circulate with an inter-bunch separation of 2.7 ns, a “good event” is produced synchronous with a crossing between two bunches at IP2. The bunches are packed by the machine RF so that the time correlation between bunches and RF is fixed. This means that a stable and

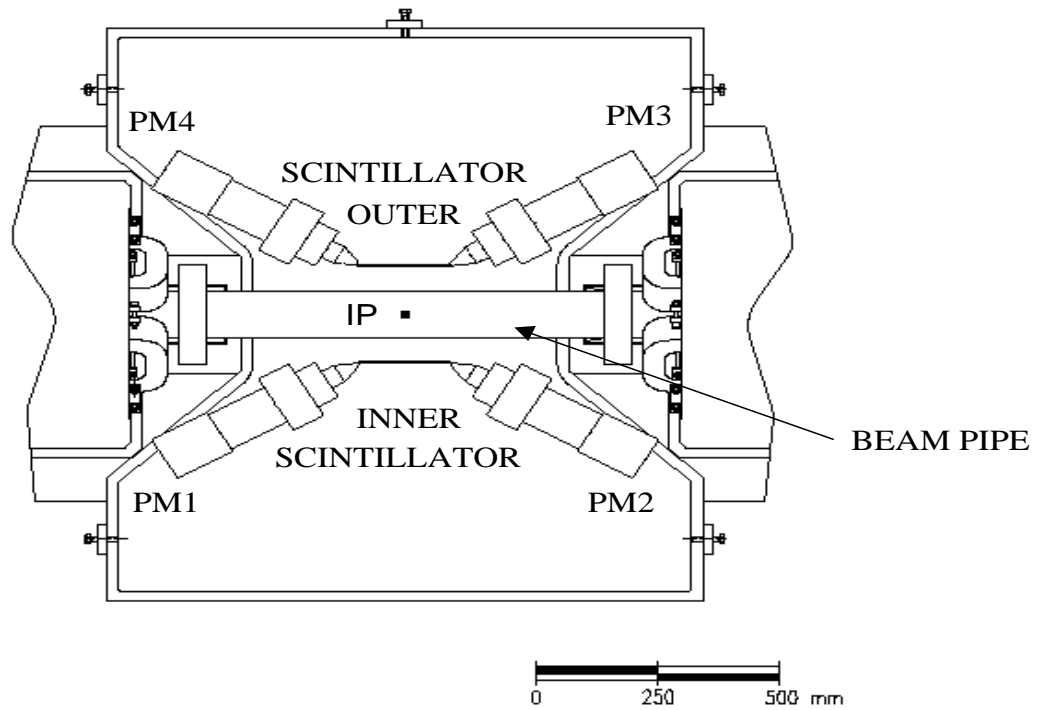


Figure 1: The Kaon Monitor experimental setup in the DEAR region at the DAΦNE interaction point (IP)

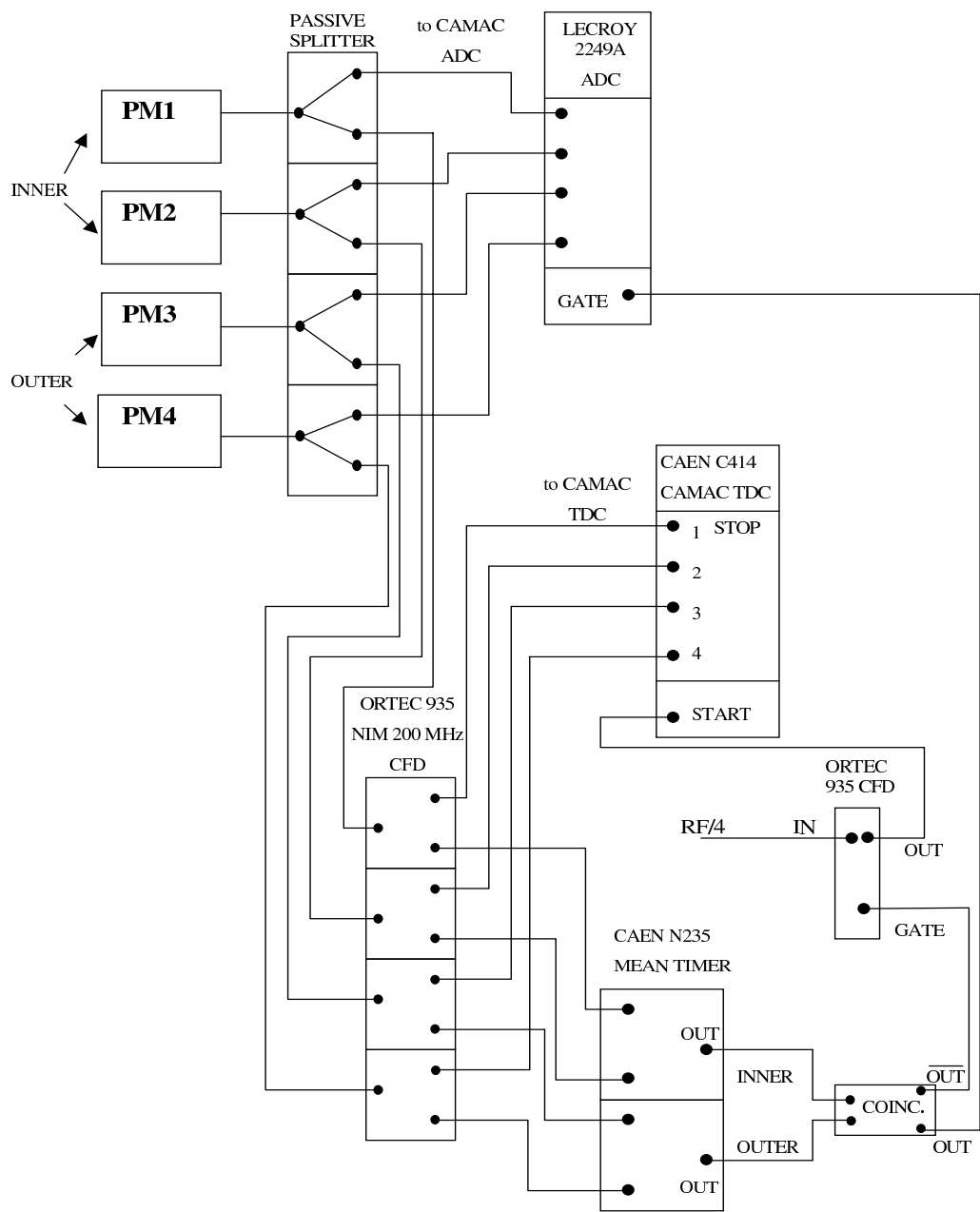


Figure 2: The Kaon Monitor electronics scheme.

reliable clock to which the TDC spectra can be referred is provided by the RF itself. However, the high rate (360 MHz) of the DAΦNE RF prevents direct utilization of such a signal to feed any TDC or to trigger a DAQ. However, there is no need to give the DAQ a trigger to start (or stop) a time-to-digital conversion each time an RF pulse arrives.

The trigger is needed only if there is a “good event”, i.e., a coincidence between the two slabs - an event that only a *few* of the bunch crossings generate. Hence the following technique is used. The RF pulses are fed to an ORTEC 935 NIM 200 MHz CFD which is inhibited unless a coincidence between the two slabs occurs. This is done by using as veto the negated output of the coincidence to inhibit the ORTEC discriminator. In such a way, the rate of the output pulses of the discriminator is reduced from the high rate of the RF to the manageable rate of the coincidences of the two slabs, but the timing is still referred to the RF clock. The output pulse of this ORTEC CFD provides the START to the TDC. The only disadvantage to this method is the possible loss of multi events in a single bunch, or the loss of events generated in subsequent consecutive bunches (i.e., bunches separated by a time interval less than the discriminator time resolution). However, this situation occurs with a negligible probability due to the experimentally measured low rate of the single arm and coincidence counts which, under normal operating conditions, are a few tens of KHz and few tens of Hz, respectively.

In practice, the gated signal of the discriminator is not the RF itself, but a proper integer submultiple,  $RF/n$ , with  $n$  selected according to the machine operating conditions. The efficiency of the RF-gated discriminator is continuously monitored by comparing the counts of its gated output with the veto signals from the coincidence to check on-line for any loss in the discriminator. No such losses were ever detected in normal operating conditions. Since the coincidence events from kaon pairs are delayed with respect to the MIPs, two peaks, separated by 1-2 ns, are expected in the TDC spectra. The time resolution of the monitor must be good enough to allow a clean separation of the kaon peak from the MIPs peak and, hence, a selection of *good* events.

As a check on the selection, the amplitude analysis of the selected good events should show a higher energy deposition, typical of the highly ionizing slow charged kaons. This last characteristic is used simply as a check, since the background events are not only due to hits of single minimum ionizing particles perpendicular to the slabs, but also to multiple and/or grazing incidence MIPs, which can deposit much higher energy in a slab with respect to a single MIP hitting the slab normally.

### 3 Tuning the monitor

After standard laboratory tests, fine tuning of the Kaon Monitor was performed in its final position at IP2, since the specific environment in which it works cannot be reproduced in the laboratory. For instance, the high voltage settings could be set only after *in situ* measurements, because the high energy deposit of a low energy charged kaon crossing the scintillator slabs could not be reproduced and the singles count rate of the scintillators in the high background region a few centimeters from the thin beam pipe of the high current collider could not be predicted. In fact, the final voltage setting selected for each phototube turned out to be lower than the optimal one obtained in the laboratory with a  $\beta$ -source, since high gains turned out to be unnecessary.

The timing of the coincidence signals of the two back-to-back slabs could be performed using the particles lost when at least one beam was circulating.

The final tuning of the delay between the RF/ $n$  signal of the ORTEC Discriminator and the gate generated by the coincidence between the mean times of the signals of the two slabs could be done only in two-beam collision conditions. The structure of the beam being periodic, it is necessary to fit the slab pulses onto the time window between the two filled bunches. For the case of the so-called “RF/2 operation mode”, the inter-bunch separation, and therefore the time window, is 5.4 ns.

After the crucial tuning of the delay between the RF/ $n$  signal and the two-slab coincidence signal, identification of the charged kaons is possible and, using the Monte Carlo evaluated detector efficiency, one can obtain an on-line measurement of the machine luminosity. The TDC spectra of each slab show two separate peaks. The peak lying at shorter times is due to the MIPs, that at longer times is due to the slow charged kaons. Setting appropriate time windows to select this second peak allows one to measure the flux of kaons and to obtain the machine luminosity.

In practice, an integer fraction of the RF signal is used. This fraction is dependent on how many bunches are actually filled, and in which way. A typical machine configuration has 45 bunches filled with the logic “yes-no yes-no”. This is called the “RF/2 operation mode”. In this case, the RF/ $n$  fraction used as input to the 200 MHz ORTEC CFD has  $n = 4$ , i.e., the RF/4 signal has a frequency of 90 MHz. The RF/4 signal reformed by the ORTEC Discriminator is used as the START for the TDC module and provides the trigger and the clock for the time measurements. To reduce the rate of this signal, the trigger is activated only if gated by the coincidence between the two scintillator slabs. The use of the RF/4 signal when the machine is operating in the “RF/2 mode” has no effect other than splitting the time spectra into two “twin” structures as shown in Fig. 3.



## 4 Experimental results

A systematic series of measurements was performed in December 2000 and May-June 2001, during DEAR data taking, to provide the experimental luminosity in the DEAR interaction point (IP2). In all these measurements the Kaon Monitor operated stably and reliably, identifying kaons with both TDC and ADC analysis and providing on-line luminosity measurements to users.

Typical correlated time and amplitude spectra are shown in Fig 3 for the inner and the outer scintillators (top and bottom figure, respectively). The bidimensional plots of the ADC mean values (of the two PMs of each slab) versus TDC show a clear separation of the kaon signal from the MIPs signal. On the TDC axis, the slow kaon signal follows the fast MIPs signals. On the ADC axis, the minimum values of the amplitudes of the signals of the two phototubes belonging to the same slab turn out, in the case of kaons, to be higher with respect to the minimum values of the MIPs signals of which the lower amplitudes are cut by the discriminator threshold. This reflects the fact that slow kaons having normal incidence to the slab lose much more energy with respect to normally impinging MIPs. The “twin” appearance of the spectra is simply the effect of the use of RF/4 as a trigger when the machine is working in the “RF/2 mode”.

In Fig. 4, the correlated spectrum of the mean time distribution of the hits on the outer slab with respect to the hits on the inner slab is shown. The region corresponding to the kaons is well separated from that corresponding to background MIPs. The kaon region is delimited by dashed lines to count on-line the particles and give a measurement of the machine luminosity.

In Fig. 5, the spectra of Fig. 3 are projected onto the TDC axis to evaluate the separation in time between kaon and MIPs peaks. It turns out to be about 1.8 ns.

In Fig 6, the distributions of the amplitudes of the signals of the PMs belonging to the inner and outer slabs, respectively, are shown. The upper plots refer to ADC spectra for all signals (kaons plus MIPs). The lower plots show the ADC spectra after putting time windows on the kaon signals (see Fig 3). After this selection, it is clearly seen that the huge low energy tail due to the MIPs disappears and a typical Landau energy loss distribution emerges, corresponding to the “monochromatic” charged kaons crossing the thin slabs. This confirms the identification of kaons.

The widths of the TDC peaks turn out to be 360 ps for kaons and 750 ps for MIPs (FWHM), showing the effectiveness of the Kaon Monitor to separate the two peaks.

The contamination of the kaon peak due to random coincidences can be estimated by looking at the mean time distribution of the kaon signal from one slab after applying a time window on the kaon signal *in the other slab*. This effect is shown in the time spectra

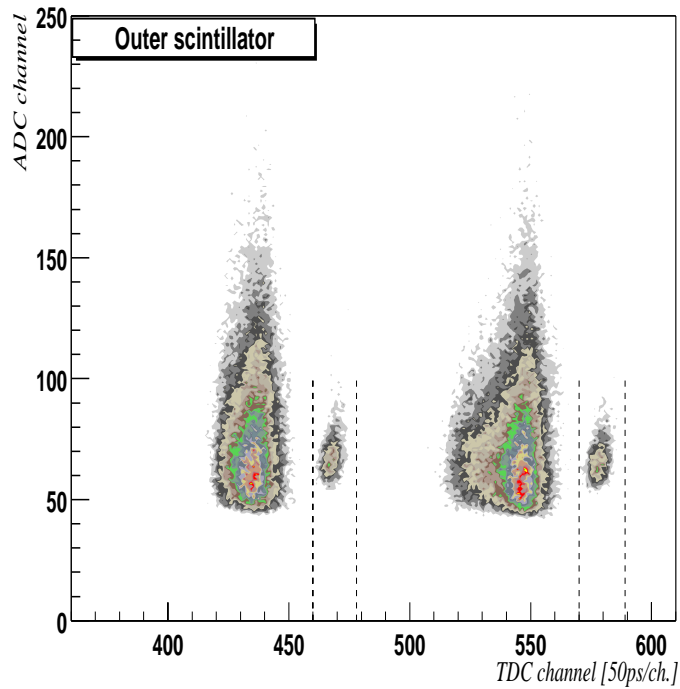
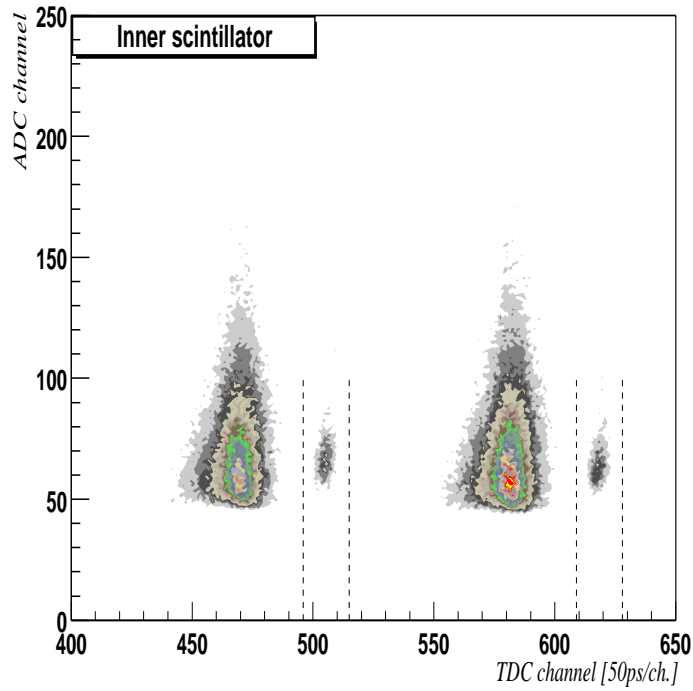


Figure 3: The correlated ADC versus TDC distributions of the inner and the outer scintillator slabs, as measured in the data taking period of December 2000.

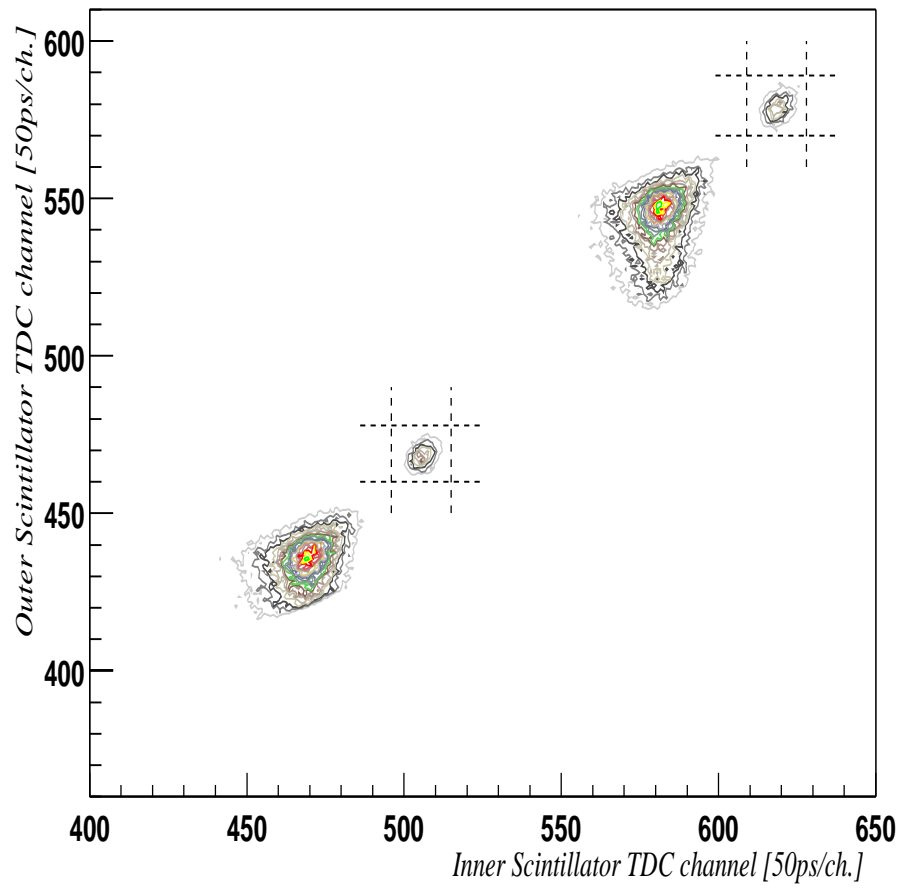


Figure 4: The correlated TDC distributions of the outer versus the inner scintillator slabs, as measured in the data taking period of December 2000.

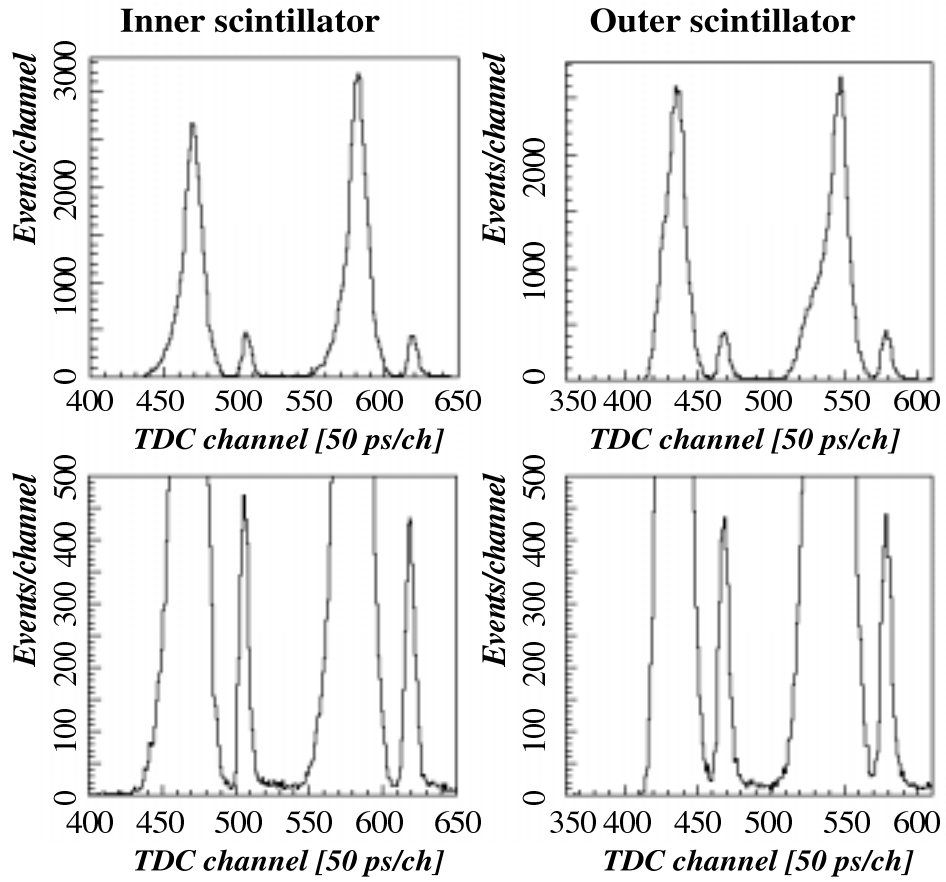


Figure 5: The TDC spectra of the inner and the outer kaon monitor scintillators. The lower spectra are a zoom of the upper ones.

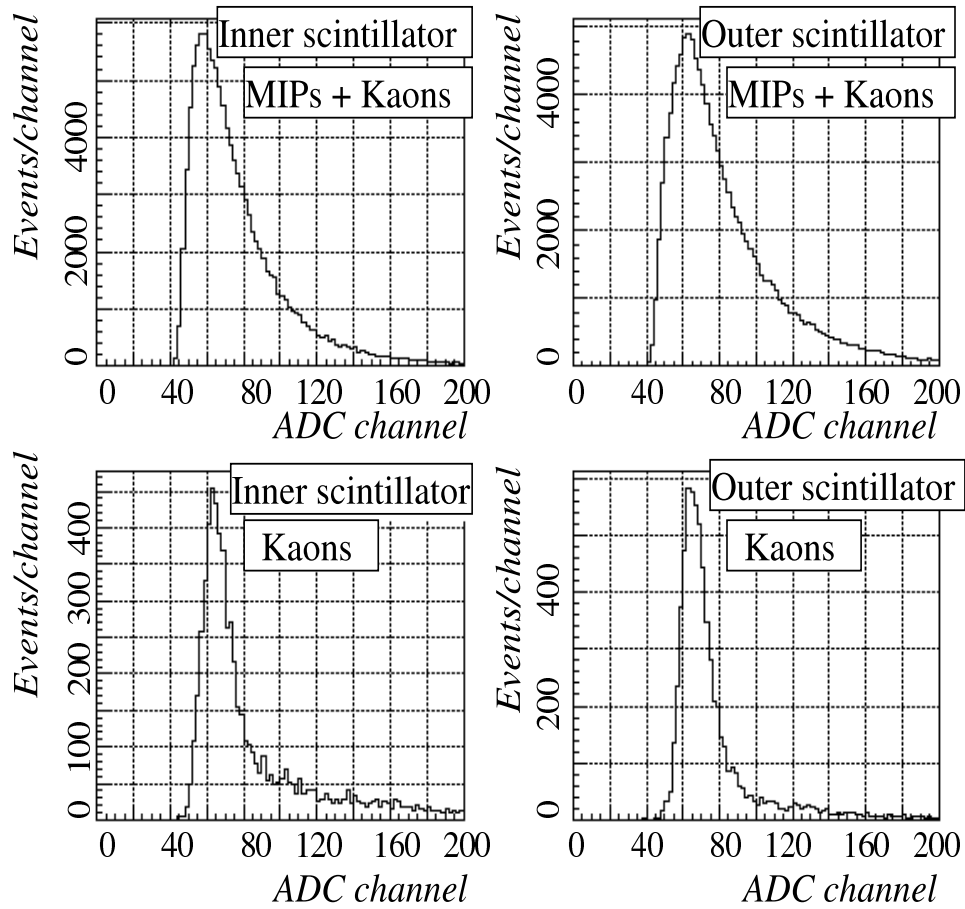


Figure 6: The ADC spectra of the inner and outer kaon monitor scintillators: the upper plots are the total (MIPs + kaons) amplitude spectra; the lower plots show the resulting ADC distributions when the cuts in the TDC spectra corresponding to slow kaons are applied.

of the inner and the outer scintillators shown in Fig 7. For both slabs, application of a kaon time window in the other slab results in a time spectrum in which, along with the kaon peak, there is a residual contamination due to MIPs background, shown by the events outside the kaon peak. When the time window for the kaons is selected *in both slabs*, this background contamination is eliminated. Only the contamination below the kaon peak remains. The number of events outside the kaon peak can be used to give an upper limit to the estimated residual contamination below the peak itself. This contamination turns out to be less than 3%.

## 5 Measurement of the DAΦNE luminosity

To measure the machine luminosity, the number of kaon pairs detected is needed. This number is obtained on-line by simultaneous selection, through time windows, of the kaon regions in the time spectra from both slabs. To allow a continuous operation of the monitor, care was taken to inhibit counting during the “dirty” periods of operation of the collider, corresponding to the injection phase. To this end a machine signal arriving 10 ms before the start of an injection inhibits DAQ for a fixed time after the last injection pulse, typically for 1-2 min.

A routine has been written to calculate on-line the number of kaons collected in a given time interval and then, knowing the *monitor efficiency*, to give the machine luminosity in IP2. This efficiency is a function of the cross section for  $\phi$ -resonance production in electron-positron collisions, of the branching ratio of  $\phi$ -decay into charged kaon pairs and of the acceptance of the monitor. The Kaon Monitor efficiency has been evaluated with a Monte Carlo simulation program which incorporates electron and positron beam energy and spatial distribution in IP2, the geometry of the detectors, the charged kaon lifetime, as well as energy loss and multiple scattering effects. The luminosity  $\mathcal{L}$  as measured by the Kaon Monitor is given by:

$$\mathcal{L} = C_{KM} \times \mathcal{R}(K^+ K^-), \quad (1)$$

where  $\mathcal{R}(K^+ K^-)$  ( $s^{-1}$ ) is the kaon pairs measured rate and  $C_{KM}$  is the Kaon Monitor efficiency:

$$C_{KM} = 7.2 \cdot 10^{30} cm^{-2}, \quad (2)$$

as given by the Monte Carlo calculations.

For  $\mathcal{L} = 10^{31} cm^{-2} s^{-1}$ ,  $\mathcal{R} = 1.4$  Hz.

For practical reasons, since the luminosity decreases with time, instead of giving the value in fixed time intervals, the number of kaon counts is preselected, taking into account the time needed to collect them. The preselected number (typically 30-50 counts)

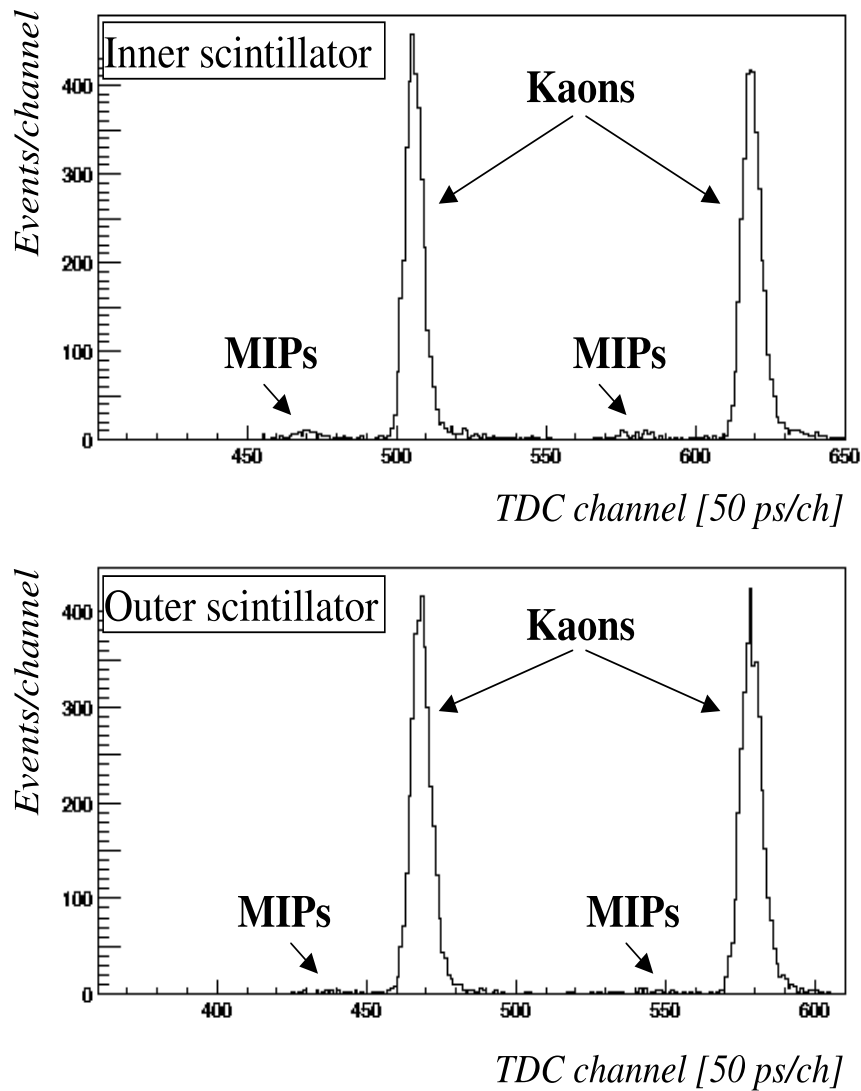


Figure 7: The TDC spectra of the inner and outer kaon monitor scintillators corresponding to kaon window selections in the time spectra of the other slab. It is worth noting that the higher MIPs contamination of the inner slab (upper plot), is related to the threefold higher single counting rate of the outer slab with respect to the inner one.

is chosen as a reasonable compromise between the statistical precision on the luminosity and the repetition frequency for giving an “instantaneous” value (a few tens of seconds at  $\mathcal{L} = 10^{31} \text{ cm}^{-2} \text{ s}^{-1}$ ).

As examples, Kaon Monitor measurements taken during periods of stable data taking in December 2000 and May-June 2001, are reported in Table 1.

The Kaon Monitor has also shown its ability to measure other machine parameters, like the outward momentum boost of decaying  $\phi$ -mesons due to the non-zero crossing angle of the electron and positron beams in DAΦNE. These results will be matters for a forthcoming paper.

## 6 Conclusions

The DEAR Kaon Monitor setup, its operation mode and its measured performance were reported. The full TDC and ADC information was collected from the detectors and the charged kaon pairs from  $\phi$ -decay could be clearly observed by means of their different arrival times with respect to the background particles.

The number of detected kaons can be transformed into machine luminosity values knowing the Kaon Monitor efficiency calculated using a Monte Carlo simulation. A software routine that, every few minutes, feeds the machine web page with the luminosity value in the DEAR interaction point was written. A hardware protection scheme enables the monitor to operate continuously inhibiting data taking during the injection phase of the collider operation.

The Kaon Monitor has been shown to perform all the tasks for which it was built, providing a count of the flux of kaons and the absolute luminosity measurement needed both for machine tuning and for the purpose of the experiment. It has also shown its ability to measure tiny effects deriving from the machine configuration.

## 7 Acknowledgements

We would like to thank Sergio Bertolucci for his constant and useful advice in tuning the Kaon Monitor.

G. Beer acknowledges support by the Natural Science & Engineering Research Council of Canada and the INFN Laboratories of Frascati.



Table 1: DAΦNE luminosity in IP2. Kaon monitor measurements of peak luminosity ( $\mathcal{L}_{peak}$ ) and integrated luminosity ( $\mathcal{L}_{int}$ ) in periods of stable data taking.

| Date and time   | Initial current $e^-$ (mA) | Initial current $e^+$ (mA) | Measurement duration (s) | Collected kaons | $\mathcal{L}_{peak}$<br>( $10^{30} cm^{-2} s^{-1}$ ) | $\mathcal{L}_{int}$<br>( $nb^{-1}$ ) |
|-----------------|----------------------------|----------------------------|--------------------------|-----------------|--|--------------------------------------|
| <b>17.12.00</b> |                            |                            |                          |                 |  |                                      |
| 2:37            | 271                        | 389                        | 2069                     | 601             | $3.79 \pm 0.42$                                      | $4.30 \pm 0.17$                      |
| 4:05            | 337                        | 376                        | 2105                     | 612             | $3.65 \pm 0.41$                                      | $4.40 \pm 0.18$                      |
| 4:51            | 343                        | 377                        | 2471                     | 783             | $5.05 \pm 0.63$                                      | $5.60 \pm 0.20$                      |
| 5:48            | 334                        | 380                        | 2105                     | 625             | $4.43 \pm 0.59$                                      | $4.50 \pm 0.18$                      |
| 6:40            | 342                        | 371                        | 2044                     | 645             | $5.98 \pm 0.68$                                      | $4.60 \pm 0.19$                      |
| <b>04.06.01</b> |                            |                            |                          |                 |  |                                      |
| 00:16           | 695                        | 630                        | 2880                     | 1434            | $6.15 \pm 0.70$                                      | $10.24 \pm 0.27$                     |
| 01:37           | 700                        | 588                        | 1860                     | 1058            | $5.62 \pm 0.66$                                      | $7.56 \pm 0.23$                      |
| 03:15           | 699                        | 586                        | 2640                     | 1458            | $5.94 \pm 0.68$                                      | $10.42 \pm 0.27$                     |
| 04:15           | 672                        | 597                        | 2100                     | 1345            | $5.50 \pm 0.64$                                      | $9.61 \pm 0.26$                      |
| 07:03           | 643                        | 549                        | 2560                     | 1393            | $5.46 \pm 0.64$                                      | $9.95 \pm 0.26$                      |
| 08:02           | 708                        | 514                        | 2400                     | 1284            | $5.09 \pm 0.63$                                      | $9.17 \pm 0.25$                      |

## 8 References

### References

- [1] S. Bianco *et al.*, (DEAR Collaboration), The DEAR case, *Rivista del Nuovo Cimento* Vol. 22, N. 11 (1999) 1-45.
- [2] G. Vignola, DAΦNE: the first  $\Phi$ -Factory, in *Proceedings of the 5th European Particle Accelerator Conference (EPAC'96)*, Sitges (Barcelona), edited by S. Myres *et al.* (Institute of Physics Publishing, Bristol and Philadelphia) 1996, p. 22.